

Plasma Waves Observed Inside Plasma Bubbles in the Equatorial F Region

15 January 1998

Prepared by

H. C. KOONS and J. L. ROEDER
Space and Environment Technology Center
Technology Operations
The Aerospace Corporation

and

P. RODRIGUEZ
Plasma Physics Division
Naval Research Laboratory
Washington, DC

Prepared for

SPACE AND MISSILE SYSTEMS CENTER
AIR FORCE MATERIEL COMMAND
2430 E. El Segundo Boulevard
Los Angeles Air Force Base, CA 90245

Engineering and Technology Group

APPROVED FOR PUBLIC RELEASE;
DISTRIBUTION UNLIMITED

19980424 112



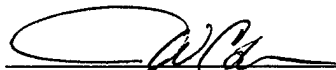
THE AEROSPACE
CORPORATION
El Segundo, California

DTIC QUALITY INSPECTED 4

This report was submitted by The Aerospace Corporation, El Segundo, CA 90245-4691, under Contract No. F04701-93-C-0094 with the Space and Missile Systems Center, 2430 E. El Segundo Blvd., Suite 6037, Los Angeles AFB, CA 90245-4687. It was reviewed and approved for The Aerospace Corporation by A. B. Christensen, Principal Director, Space and Environment Technology Center. Maj. J. W. Cole was the project officer for the Mission-Oriented Investigation and Experimentation Program (MOIE) program.

This report has been reviewed by the Public Affairs Office (PAS) and is releasable to the National Technical Information Service (NTIS). At NTIS, it will be available to the general public, including foreign nationals.

This technical report has been reviewed and is approved for publication. Publication of this report does not constitute Air Force approval of the report's findings or conclusions. It is published only for the exchange and stimulation of ideas.



J. W. Cole, Maj. USAF
SMC/AXES

| REPORT DOCUMENTATION PAGE | | | Form Approved OMB No. 0704-0188 | |
|---|---|--|---|----------------------------------|
| Public reporting burden for this collection of information is estimated to average 1 hour per response, including the time for reviewing instructions, searching existing data sources, gathering and maintaining the data needed, and completing and reviewing the collection of information. Send comments regarding this burden estimate or any other aspect of this collection of information, including suggestions for reducing this burden to Washington Headquarters Services, Directorate for Information Operations and Reports, 1215 Jefferson Davis Highway, Suite 1204, Arlington, VA 22202-4302, and to the Office of Management and Budget, Paperwork Reduction Project (0704-0188), Washington, DC 20503. | | | | |
| 1. AGENCY USE ONLY (Leave blank) | | 2. REPORT DATE 15 January 1998 | | 3. REPORT TYPE AND DATES COVERED |
| 4. TITLE AND SUBTITLE Plasma Waves Observed Inside Plasma Bubbles in the Equatorial F Region | | | 5. FUNDING NUMBERS F04701-93-C-0094 | |
| 6. AUTHOR(S) Koons, H. C.; Roeder, J. L.; and Rodriguez, P. | | | | |
| 7. PERFORMING ORGANIZATION NAME(S) AND ADDRESS(ES) The Aerospace Corporation Technology Operations El Segundo, CA 90245-4691 | | | 8. PERFORMING ORGANIZATION REPORT NUMBER TR-98(8570)-1 | |
| 9. SPONSORING/MONITORING AGENCY NAME(S) AND ADDRESS(ES) Space and Missile Systems Center Air Force Materiel Command 2430 E. El Segundo Blvd. Los Angeles Air Force Base, CA 90245 | | | 10. SPONSORING/MONITORING AGENCY REPORT NUMBER SMC-TR-98-03 | |
| 11. SUPPLEMENTARY NOTES | | | | |
| 12a. DISTRIBUTION/AVAILABILITY STATEMENT Approved for public release; distribution unlimited | | | 12b. DISTRIBUTION CODE | |
| 13. ABSTRACT (Maximum 200 words) Plasma waves have been detected within and around density depletions in the topside equatorial F region by the electric and magnetic field sensors of the Extremely Low Frequency Wave Analyzer (ELFWA) instrument which is part of the Low-Altitude Satellite Studies of Ionospheric Irregularities experiment on the Combined Release and Radiation Effects Satellite. The plasma waves include both electrostatic waves that have a small magnetic field component and electromagnetic waves propagating in the extraordinary mode. Thus they are not simply zero-frequency irregularities as generally assumed by previous investigators who were working without the benefit of high-sensitivity ac magnetic field measurements. The waves exhibit no resonances or cutoffs at characteristic frequencies of the plasma within the range of the ELFWA which is 2-125 Hz. They occur from late evening to early morning primarily at altitudes around 400-500 km. An example has been observed as high as 1500 km. The waves are associated with plasma depletions from a factor of 2 to a factor of 80 less than the surrounding density. The observations indicate that the waves are related to equatorial spread F. | | | | |
| 14. SUBJECT TERMS Electromagnetic waves Ionosphere Electrostatic waves Spread F F region | | | 15. NUMBER OF PAGES 9 | |
| | | | 16. PRICE CODE | |
| 17. SECURITY CLASSIFICATION OF REPORT Unclassified | 18. SECURITY CLASSIFICATION OF THIS PAGE Unclassified | 19. SECURITY CLASSIFICATION OF ABSTRACT Unclassified | 20. LIMITATION OF ABSTRACT | |

Plasma waves observed inside plasma bubbles in the equatorial F region

H. C. Koons and J. L. Roeder

Space and Environment Technology Center, The Aerospace Corporation, Los Angeles, California

P. Rodriguez

Plasma Physics Division, Naval Research Laboratory, Washington, D. C.

Abstract. Plasma waves have been detected within and around density depletions in the topside equatorial F region by the electric and magnetic field sensors of the Extremely Low Frequency Wave Analyzer (ELFWA) instrument which is part of the Low-Altitude Satellite Studies of Ionospheric Irregularities experiment on the Combined Release and Radiation Effects Satellite. The plasma waves include both electrostatic waves that have a small magnetic field component and electromagnetic waves propagating in the extraordinary mode. Thus they are not simply zero-frequency irregularities as generally assumed by previous investigators who were working without the benefit of high-sensitivity ac magnetic field measurements. The waves exhibit no resonances or cutoffs at characteristic frequencies of the plasma within the range of the ELFWA which is 2–125 Hz. They occur from late evening to early morning primarily at altitudes around 400–500 km. An example has been observed as high as 1500 km. The waves are associated with plasma depletions from a factor of 2 to a factor of 80 less than the surrounding density. The observations indicate that the waves are related to equatorial spread F .

Introduction

In this paper we describe measurements of the magnetic and electric components of naturally occurring extremely low frequency (ELF) plasma waves associated with density depletions in the nighttime, topside, equatorial F region. The observations were made by the Low-Altitude Satellite Studies of Ionospheric Irregularities (LASSII) experiment [Rodriguez, 1992] on the Combined Release and Radiation Effects (CRRES) satellite. The objective of the LASSII experiment is to determine the mechanisms responsible for naturally occurring and artificially created plasma irregularities in the low-latitude ionosphere.

The LASSII experiment consists of a pulsed plasma probe (P^3), an extremely low frequency wave analyzer (ELFWA), and a quadrupole ion mass spectrometer (QIMS). The plasma wave measurements we report were made by the ELFWA, and the electron density measurements were made by the P^3 . The ELFWA is designed to measure both the electric and the magnetic field components of electromagnetic and electrostatic plasma waves at frequencies from 2 to 125 Hz.

Previous spacecraft [Kelley and Mozer, 1972; Holtet et al., 1977; Aggson et al., 1993] and rocket [Kelley et al., 1982; Hysell et al., 1994] measurements of plasma waves and irregularities associated with spread F in the topside equatorial F region have used sensitive electric field detectors. However, they have either made no magnetic field measurements at all or they used aspect magnetometers that do not have sufficient sensitivity to measure the magnetic field components of ELF plasma waves. Hence previous measurements have been unable to determine if the waves they detected were electromagnetic. Under those circumstances most investigators assumed that the ac electric

field fluctuations they observed were due to the antenna passing through a region of nonpropagating or zero-frequency irregularities [Holtet et al., 1977; Aggson et al., 1993]. Kelley and Mozer [1972] inferred the electrostatic nature of the waves that they observed at the equator from the fact that another satellite detected no magnetic component for "similar" emissions at high latitudes.

Kelley et al. [1979] reported a single spacecraft observation of ELF electromagnetic waves associated with equatorial spread F below the F peak. The electric field signals were measured in the 4–16 Hz and 256–1024 Hz channels, and the magnetic field was measured in a single channel at 999 Hz.

Theories for the formation of spread F phenomena are extensive (for a review, see Kelley [1989, chapter 4]). It is commonly assumed that the generalized Rayleigh-Taylor instability occurs in the nighttime, bottomside F region to produce large-scale density depletions. These depletions convect upward, resulting in sharp density gradients in the topside F region. The large-scale features are thought to eventually generate a spectrum of small-scale irregularities via several processes. Candidate mechanisms include the turbulent cascade of long wavelength irregularities to short wavelength irregularities and the electrostatic gradient drift instability. Both of these processes produce only density variations. These density variations are detected as ac voltage variations on an antenna moving through them. There are no accompanying magnetic field variations. The observations reported here of electromagnetic waves and electrostatic waves (with small magnetic components) propagating at a nonzero angle with respect to the geomagnetic field in the topside spread F region generally contradict existing theories of spread F formation.

Instrument Overview

Spacecraft. The CRRES spacecraft is a spinning spacecraft with a perigee of 350 km, an apogee of 33,580 km, an

inclination of 18° , an orbital period of 9.87 hours, and a spin period of 30 s. This orbit provided only limited opportunities for the LASSII instruments to perform measurements in the ionosphere. In addition, LASSII measurements were further constrained by orbital operations which limited LASSII's duty cycle. The primary region of interest was the nighttime sector of the orbit and especially the dawn and dusk transitions, at altitudes below 3000 km. The CRRES orbit precessed in local time with an apparent period of 1.5 years. When perigee was on the nightside, LASSII performed measurements every other orbit below an altitude of 3000 km. When perigee was on the dayside, measurements were performed every fourth orbit below 1000 km. This schedule yielded a total of 264 perigee data acquisitions between July 28, 1990, and October 11, 1991, when the CRRES mission ended.

Extremely low frequency wave analyzer. The ELFWA measures single-axis electric field spectra and amplitudes from 2 to 250 Hz and single-axis magnetic field spectra and amplitudes from 2 to 125 Hz. Two antennas, two preamplifiers, and two electronics boxes comprise the instrument. The electric field sensor consists of two spherical probes each 6.35 cm in diameter on booms 190.5 cm long deployed above the spacecraft. The probes are separated by 4.5 m. The signals from the two probes are differenced in the E field electronics package to provide a single-axis electric field measurement which rotates in the spin plane of the spacecraft.

The magnetic field antenna is a 50-cm-diameter, 1600-turn loop deployed on a 2-m boom. The frequency response of the B field antenna increases 6 dB per octave in the 12.5- to 125-Hz frequency range. The preamplifier has been frequency-compensated with 6 dB per octave bass boost to produce a flat frequency response from the antenna and preamplifier combination from 10 to 125 Hz. The single-axis magnetic antenna rotates in the spin plane of the spacecraft. However, the sensed component is not parallel to the electric field component measured by the electric antenna. The angle between the magnetic and electric components is 32° .

The E field and the B field signals are sampled at evenly spaced intervals 250 times s^{-1} providing a 125-Hz Nyquist frequency for the signal from each antenna. Each of the electronics packages has independent gain settings of 0, -20, and -40 dB and two modes, linear and automatic gain control (AGC). The dynamic range is 48 dB in the linear mode and approximately 90 dB in the AGC mode at one gain setting. The decay time constant of the AGC circuit is approximately 2 s, and the AGC voltage is monitored once every 2 s. For the observations reported in this paper the experiment took data in the AGC mode with the gain set at 0 dB. The sensitivity, corresponding to 0.02 V (1 bit) output from the electronics packages, is $9.9 \times 10^{-7} \text{ V m}^{-1}$ from the electric antenna and 0.2 pT from the magnetic antenna. The broadband signal (i.e., the total signal in-band from 2 to 125 Hz) is also averaged and recorded each second. A more complete description of the instrument is given by Koons *et al.* [1992].

Pulsed plasma probe. The Langmuir probe instrument P³ operates as two pulsed plasma probes and measures ionospheric electron densities, temperatures, and fluctuations of the plasma. The experiment consists of two cylindrical Langmuir probes, two preamplifiers, and two electronics boxes. Each of the Langmuir probes is made of tungsten wire 20 cm long and 0.09 cm in diameter, mounted on the end of a boom about 2 m in length. Normally, one probe was biased to measure electron currents, and the other was biased to measure ion

currents. The instrument was designed to make two types of measurements: a traditional probe current as a function of probe voltage measurement to determine the electron density and temperature and a current measurement at constant bias voltage. The latter provides a higher time resolution measurement of the electron density including density fluctuations to 100 Hz. In the traditional mode the fixed bias voltage is +5.5 V, and the sweep bias voltage sweeps from -3.0 to +6.0 V. The sweep period is then commandable to either 0.7 or 2.5 s per sweep. In the saturation current mode a fixed bias of +5.5 V was used for the electron probe. The electron density measurements reported in this paper were obtained with the probe operating at a constant bias level. A more complete description of the instrument is given by Baumback *et al.* [1992].

Description of Data

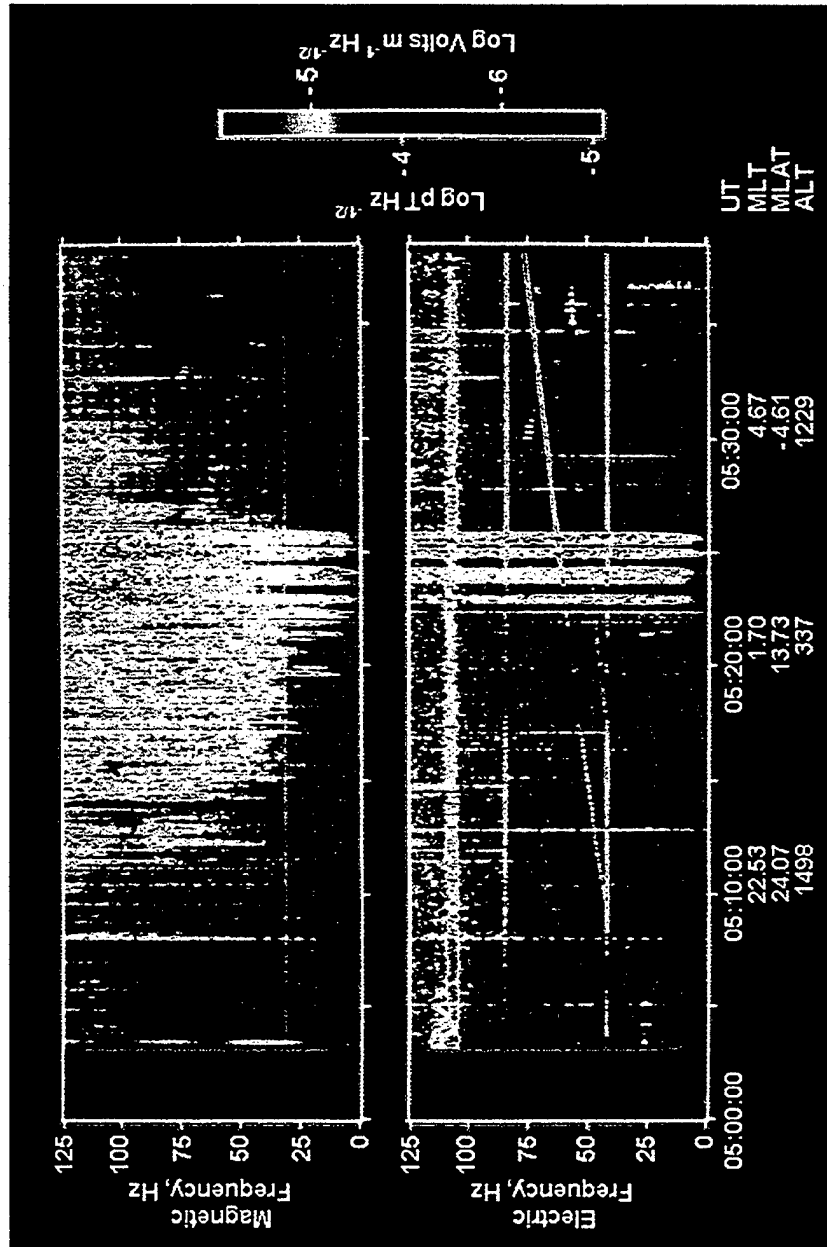
The primary data for this study consist of color spectrograms of the ELF electric and magnetic fields for each of the 264 perigee acquisitions between July 28, 1990, and October 11, 1991, for which data were collected by the LASSII instruments. The electric field spectrograms cover the frequency range from 2 to 125 Hz when the magnetic field data were collected and 2 to 250 Hz when only the electric field data were collected.

Evidence for electromagnetic waves was found on 37 of the 264 spectrograms. In all, 53 such events were found on the 37 spectrograms.

We have determined that the largest amplitude waves are primarily electrostatic with a small magnetic component. However, electromagnetic waves propagating in the extraordinary mode were also observed. Both the electrostatic and the electromagnetic waves appear to be related to density depletions, and they may play an important role in the kilometer scale processes occurring within spread F regions. In the remainder of the paper we describe the characteristics and occurrence of these waves.

Example event. We will first describe the characteristics of an example event that was observed on October 7, 1991. The spectrogram in Plate 1 shows a series of field enhancements between 0522 and 0526 UT. The characteristic feature in the spectrum is the intense, wideband signal that crosses essentially the entire frequency range from 10 to 125 Hz. The feature can be seen in both the electric field and the magnetic field components. Each vertical band is about 30 s wide, and four bands can be easily discerned. At 0524 UT the spacecraft was at an altitude of 453 km and a magnetic latitude of 6.2°N moving with a velocity of 10 km s^{-1} . The local time was 0245. The total width in time of the four events is 156 s. Thus they were observed for a total distance of 1560 km along the track of the spacecraft. The length of the individual features ranges from 240 to 480 km along the track. This is essentially the horizontal size of the features because the vehicle velocity vector was pointing only 10° above the horizontal at this time. Figures 1a and 1b show the broadband intensity within the band of the receivers for the entire perigee pass shown in Plate 1. The enhancements between 0522 and 0526 UT stand out several tens of decibels above the background in the magnetic channel (Figure 1b), and there is essentially no background at the receiver gain setting used for the electric channel (Figure 1a). These enhancements dominate the electric field data during this data acquisition.

The cause of the background in the magnetic channel is not known. It may be electromagnetic interference, or it may be



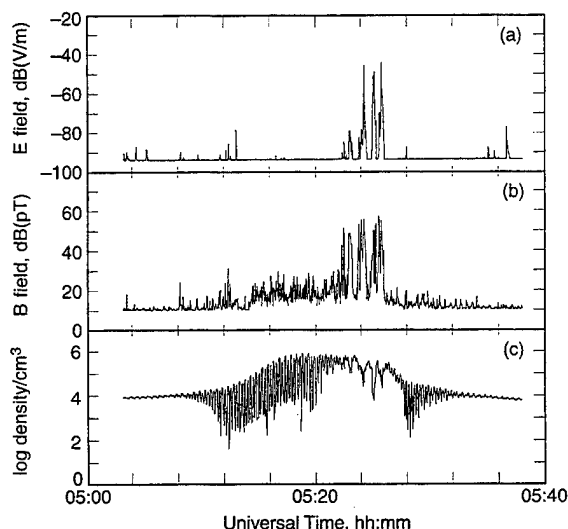


Figure 1. The broadband field intensities and plasma density measured as a function of time during the perigee pass around 0520 UT, October 7, 1991. (a) The ac electric field, (b) the ac magnetic field, and (c) the electron density. The strong modulation of the electron density is caused by the rotation of the probes through the ram and wake of the spacecraft. The values on the y axis apply to the upper envelope of the modulated spectrum.

the magnetic component of an electromagnetic wave propagating in a mode for which the electric field component is below the noise level of the broadband electric field measurement. The background in the magnetic channel shows little structure on the color spectrogram in Plate 1 and has a low-frequency cutoff above the oxygen ion gyrofrequency which was 24.8 Hz at 0520 UT.

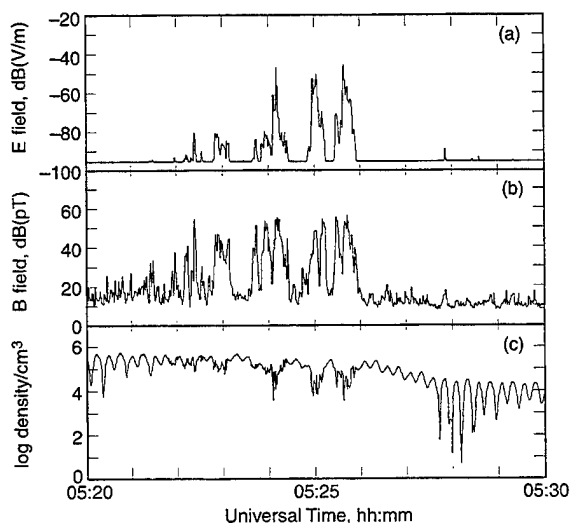


Figure 2. The broadband intensity measured as a function of time within the 125-Hz bandwidth of the ELFWA. The data were taken during the perigee pass around 0520 UT, October 7, 1991. This is an enlargement of the time period from Figure 1 when the most intense emissions were observed.

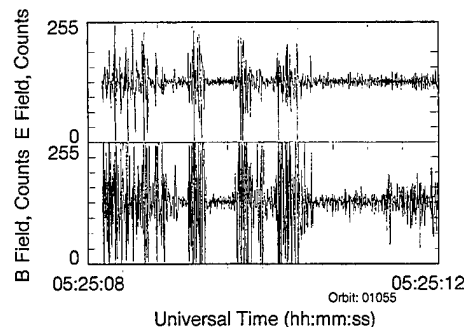


Figure 3. Raw digital data showing the close relationship in time between the signals on the electric field antenna and on the magnetic field antenna.

Figures 2a and 2b show the broadband signal within the band of the receivers for the 10-m time period approximately centered on this event. It shows the general correlation in time on this scale of the features in the electric and the magnetic channels. Although the magnetic data appear to contain more structure, there is usually a corresponding maxima in both channels almost simultaneously.

Figure 3 shows the waveform data from each antenna for the 4-s period between 0525:08 and 0525:12 UT. The high degree of temporal relationship between the waveforms from the two channels is convincing evidence that these waves have both electric and magnetic components.

Figure 1c shows the signal from the Langmuir probe for this data acquisition. At the time the Langmuir probe was operating at a constant positive bias to collect electrons. The modulation of the signal is caused by the changing aspect angle of the collecting surface of the probe with respect to the ram direction and with respect to the geomagnetic field. The slow variation of the envelope is caused by the slow change of these aspect angles along the orbit. The rapid fluctuations are caused by the change in the aspect angles as the spacecraft rotates. At the higher altitudes near the beginning and end of the data acquisition shown in Figure 1 the Debye length in the plasma is ≈ 2 cm, and the plasma sheath around the probe is comparable to the dimensions of the probe. Under those conditions the aspect dependent modulation is small. Near perigee the sheath is almost an order of magnitude smaller, and then the modulation is large. The electron density is determined from the upper envelope of the signal. The upper envelope represents the maximum current collected in a rotation period. This occurs when the probe axis is most nearly perpendicular to the ram and to the geomagnetic field. The actual value determined from the upper envelope is a lower limit to the density since exact perpendicularity to both the ram and the geomagnetic field is seldom realized simultaneously.

Coincident in time with the three large electric field events in Figure 1 around 0525 UT are noticeable decreases in the Langmuir probe signal. Figure 2 shows an expanded view of the data for this time period. From 0521 to 0527 UT the modulation of the signal caused by the rotation of the spacecraft is relatively small. Superimposed on this modulation are a number of irregular decreases in the signal from the probe. These decreases are actual decreases in the electron density. The density obtained from the upper envelope of the curve around 0525 UT is $8 \times 10^{11} \text{ m}^{-3}$. The signal at the minima in

the deeper depletions corresponds to a density of 10^{10} m^{-3} . This represents density depletions of a factor of 80 that are generally coincident with the larger ELF events. The modulation of the signal from the Langmuir probe is expected to be smaller within a density depletion because the plasma sheath surrounding the probe is large. These electron density depletions resemble the ion density depletions known as plasma bubbles observed by Ogo 6 [Hanson and Santani, 1973] and by the Atmospheric Explorer satellite AE-C [McClure et al., 1977] in both the depth of the depletion and the east-west size of the bubbles.

The correspondence between the electric field intensity and the density depletions that we have observed is essentially the same as reported by Aggson et al. [1993]. They attributed the electric field signals on the San Marco satellite to spatial irregularities along the trajectory of the spacecraft with dimensions varying from 1 m to 1 km in the east-west direction. They show that at wavelengths greater than the ion gyroradius the rms ac electric field amplitude closely tracked variations in the dc electric field. There have been no previous reports of measurements of ELF magnetic fields associated with density depletions in the topside, equatorial *F* region.

Wave modes. The density depletions complicate the determination of the wave modes for the observed ELF signals. The wave mode for an electromagnetic wave can be determined from its index of refraction in the plasma. The index of refraction for a wave can be estimated from the ratio cB/E , where c is the speed of light, B is the magnetic field intensity, and E is the electric field intensity. Because the antenna system has only one axis per component, the spacecraft is rotating, and the duration of the waves is short compared with the spin period of the spacecraft, this gives only a crude estimate of the index of refraction. However, this estimate is normally adequate to distinguish electromagnetic waves from predominantly electrostatic waves.

For the index of refraction estimate we use the broadband data rather than the waveform sampled data because the calibration of the former does not depend on the response of the AGC circuit to rapidly varying signals as does the latter. Table 1 contains the values for B and E and the ratio cB/E obtained

Table 1. Maximum Electric and Magnetic Field Intensities for the ELF Events Observed During Orbit 1055 on October 7, 1991

| Universal Time | E , dBV m^{-1} | B , dBpT | cB/E |
|----------------|------------------------------|---------------|--------|
| 0508:03 | -90.0 | 24.0 | 150 |
| 0512:02 | -89.0 | 26.0 | 169 |
| 0512:16 | -86.0 | 31.0 | 212 |
| 0522:12 | -90.5 | 42.5 | 1340 |
| 0522:21 | -78.8 | 56.0 | 1649 |
| 0522:49 | -79.2 | 48.4 | 720 |
| 0523:41 | -82.4 | 52.9 | 1746 |
| 0523:53 | -77.9 | 55.1 | 1340 |
| 0524:04 | -59.8 | 55.6 | 177 |
| 0524:07 | -45.3 | 56.5 | 37 |
| 0524:55 | -50.7 | 50.6 | 35 |
| 0525:08 | -67.9 | 55.6 | 449 |
| 0525:27 | -69.3 | 56.9 | 613 |
| 0525:37 | -44.0 | 54.7 | 26 |
| 0525:40 | -55.3 | 58.3 | 144 |

ELF, extremely low frequency; E , electric field; B , magnetic field; c , speed of light.

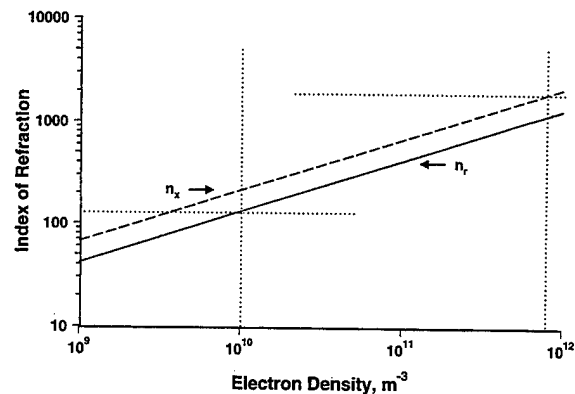


Figure 4. The index of refraction at 40 Hz for the right-hand mode n_r and the extraordinary mode n_x as a function of the plasma electron density.

at selected local maxima in the broadband data throughout the perigee acquisition on Orbit 1055.

The first three events in Table 1 occurred above 1000 km. They are relatively short (less than 2 s long) and show the characteristic harmonic bands associated with satellite observations of multiple stroke lightning [Shaw and Gurnett, 1971]. This pattern of vertical dashes on the spectrogram is especially noticeable in Plate 1 for the lightning event at 0508:03 UT. They are caused by lightning-generated waves traveling in either the right-hand or the extraordinary propagation mode. At the locations where they were observed, the indices of refraction for the two electromagnetic modes were too close to distinguish them apart using the broadband data, and the duration of the signals was too short to distinguish the modes using the rotating antenna pattern to determine the direction of the components with respect to the geomagnetic field.

The peaks at 0524:07, 0524:55, and 0525:37 UT have indices of refraction below 40 and thus are predominantly electrostatic. These are the three events which stand out in intensity above the others in the electric field data shown in Figure 1a. It is interesting to note in Table 1 that it is a larger electric field that yields the lower index of refraction estimate. The magnetic field for all the events in Table 1 after 0522:21 UT has only a 16-dB intensity range from +42.5 to +58.3 dBpT. The electric field, however, has a 46.5-dB range from -90.5 to -44.0 dBV $\text{m}^{-1} \text{ Hz}^{1/2}$.

Figure 4 shows a graph of the index of refraction for the extraordinary and the right-hand electromagnetic modes as a function of the electron density. The values are calculated for the magnetic field intensity at the satellite at 0525 UT. The vertical dotted lines in the figure identify the upper and lower density limits obtained from the Langmuir probe data around that time. The horizontal dotted lines identify the extreme upper and lower limits for the indices of refraction based on those density limits. The index of refraction can range from 211 to 1884 for the extraordinary mode n_x and from 131 to 1167 for the right-hand mode n_r . Since the three extreme low values for cB/E in Table 1 are significantly less than the lowest expected values for n_x and n_r , they must correspond to electrostatic waves with a small magnetic component. These waves have the same characteristics as those that were generated by the CRRES low-altitude chemical releases [Koons and Roeder, 1995]. The waves generated by the chemical releases had val-

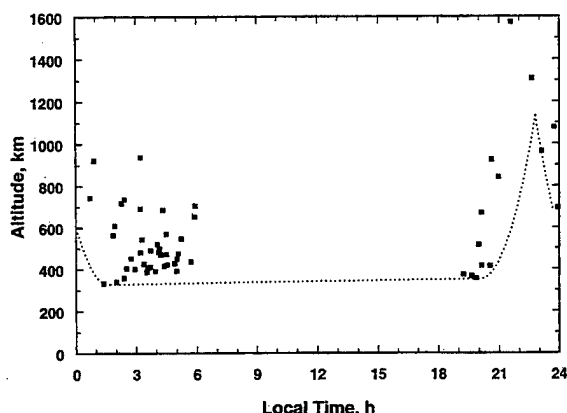


Figure 5. The locations in altitude and local time where the plasma waves associated with plasma bubbles in the equatorial *F* region were observed. The dotted line is the lower limit of the region accessible to the CRRES orbit during the 15 months of observations.

ues of cB/E that ranged from 21 to 429. Because the ambient electron densities for the chemical releases were roughly the same as the density for this orbit near but outside of the depleted regions, the indices of refraction for the chemical releases for the electromagnetic modes would be much higher. The small magnetic field component is consistent with the transverse magnetic field of primarily electrostatic ion-acoustic waves which are propagating at a finite angle with respect to the geomagnetic field.

The signals at 0522:12, 0522:21, 0523:41, and 0523:53 UT have values of cB/E between 1340 and 1746. Those values are consistent with the index of refraction for the extraordinary mode at the higher electron densities outside of the depleted regions. The signals at 0522:49, 0524:04, 0525:08, 0525:27, and 0525:40 UT have values of cB/E between 144 and 720. That is consistent with the expected values of both n_x and n_z within the density depletions. Since the waves outside of the depletions appear to be propagating in the extraordinary mode, it is likely that the waves within the depletions are also propagating in the extraordinary mode.

The right-hand and extraordinary modes can normally be distinguished by the direction of the field components with respect to the dc magnetic field. However, it is not possible to determine the directions of the electric and magnetic field vectors with respect to the geomagnetic field for the emissions reported here with the ELFWA because each antenna has only one axis and the temporal variation of the signal is too rapid to even determine the direction of the field in the spin plane.

Plasma Wave Occurrence

These waves were not observed uniformly in space or time during the CRRES mission. They were only observed in the nightside ionosphere between 1900 and 0600 LT. Figure 5 shows a scatterplot of the wave observations in altitude and local time. The dotted line in Figure 5 is the lower limit of the CRRES observations. At launch, perigee occurred at 2000 LT. By the end of the mission, perigee had rotated to 0200 LT. This left a premidnight gap in coverage as shown in the figure. The waves occur throughout the altitude range of the LASSII observations from perigee, which varied from 327 to 350 km

during the 15-month mission, up to 1000 km. Two isolated events were also detected above that at altitudes of 1308 and 1574 km. Although there is reasonably complete coverage of the dayside ionosphere between the altitudes of 350 and 1000 km, no waves with these characteristics were detected on the dayside. The peak of the occurrence distribution is between 400 and 500 km. Most of the observations in that range occurred between 0300 and 0600 LT. The waves are observed on the topside of the *F* region between sunset and sunrise. The perigee of the CRRES spacecraft was too high to make observations below the peak of the *F* layer. The overall morphology of these ELF plasma waves is similar to the morphology of equatorial spread *F* [Calvert and Schmid, 1964; Singleton, 1968].

In order to determine if the observations are related to field-aligned plasma depletions we also mapped the observations along the geomagnetic field line to the equatorial plane [Mendillo and Tyler, 1983]. A scatterplot of the equatorial altitude of the magnetic field line versus local time showed significantly more scatter in altitude than the data in Figure 5 for the postmidnight emissions and about the same scatter for premidnight emissions. For the postmidnight emissions the observation altitudes better organize the data than the equatorial altitudes of the magnetic field lines on which the observations were made. This implies that the emissions are probably not occurring throughout the entire region occupied by field-aligned plasma depletions but are primarily associated with plasma depletions in the altitude range from 350 to 800 km. We emphasize that the data points in Figure 5 represent observations of waves associated with density depletions and that the distribution shown in Figure 5 is not to be construed as the distribution of plasma bubbles in altitude and local time.

Summary

Four categories of short-duration broadband ELF emissions were observed during the data acquisition on October 7, 1991: (1) lightning-generated emissions above 1000 km, (2) predominantly electrostatic waves within density depletions, (3) extraordinary electromagnetic waves propagating in the ambient medium outside of the density depletions, and (4) extraordinary electromagnetic waves propagating within the density depletions. The wave modes are identified by the ratio cB/E .

The spectra of the latter three categories are essentially the same. They are broadband with no resonances or cutoffs at characteristic frequencies of the plasma within the range of the ELFWA.

The waves are not simply zero-frequency irregularities as generally assumed by previous investigators; they are associated with plasma depletions from a factor of 2 to a factor of 80 less than the surrounding density. The observations indicate that both the electrostatic and the electromagnetic waves are associated with equatorial spread *F*.

Acknowledgments. We thank M. Baumbach of NRL for the electron density data from the Pulsed Plasma Probe experiment on LASSII. We also acknowledge the efforts of W. B. Harbridge, S. Imamoto, D. Katsuda, P. Lew, D. Mabry, and W. Wong in the fabrication, testing, and integration of the ELFWA instrument. This work was supported by the Space and Missile Systems Center, Air Force Materiel Command under contract F04701-93-C-94.

The Editor thanks M. Parrot and another referee for their assistance in evaluating this paper.

References

- Aggson, T. L., W. B. Hanson, F. A. Herrero, N. C. Maynard, R. F. Pfaff, J. L. Saba, and R. T. Tsunoda, Equatorial electric field observations, *Adv. Space Res.*, 13(1), 271–291, 1993.
- Baumback, M., P. Rodriguez, D. N. Walker, and C. L. Siefring, LASSII Pulsed Plasma Probe on CRRES, *J. Spacecr. Rockets*, 29, 607–609, 1992.
- Calvert, W., and C. W. Schmid, Spread F observations by the Alouette topside sounder satellite, *J. Geophys. Res.*, 69, 1839–1852, 1964.
- Hanson, W. B., and S. Santani, Large N_i gradients below the equatorial F peak, *J. Geophys. Res.*, 78, 1167–1173, 1973.
- Holtet, J. A., N. C. Maynard, and J. P. Heppner, Variational electric fields at low latitudes and their relation to spread- F and plasma irregularities, *J. Atmos. Terr. Phys.*, 39, 247–262, 1977.
- Hysell, D. L., M. C. Kelley, W. E. Swartz, R. F. Pfaff, and C. M. Swenson, Steepened structures in equatorial spread F , 1, New observations, *J. Geophys. Res.*, 99, 8827–8840, 1994.
- Kelley, M. C., *The Earth's Ionosphere*, chap. 4, Academic, San Diego, Calif., 1989.
- Kelley, M. C., and F. S. Mozer, A satellite survey of vector electric fields in the ionosphere at frequencies of 10 to 500 Hertz, 3, Low-frequency equatorial emissions and their relationship to ionospheric turbulence, *J. Geophys. Res.*, 77, 4183–4189, 1972.
- Kelley, M. C., J. A. Holtet, and B. T. Tsurutani, Observations of ELF electromagnetic waves associated with equatorial spread F , *Planet. Space Sci.*, 27, 127–130, 1979.
- Kelley, M. C., R. Pfaff, K. D. Baker, J. C. Ulwick, R. Livingston, C. Rino, and R. Tsunoda, Simultaneous rocket probe and radar measurements of equatorial spread F —Transitional and short-wavelength results, *J. Geophys. Res.*, 87, 1575–1588, 1982.
- Koons, H. C., J. L. Roeder, and W. B. Harbridge, Extremely low frequency wave analyzer, *J. Spacecr. Rockets*, 29, 606–607, 1992.
- Koons, H. C., and J. L. Roeder, Observations of ELF fields near the low-altitude CRRES chemical releases, *J. Geophys. Res.*, 100, 5801–5810, 1995.
- McClure, J. P., W. B. Hanson, and J. H. Hoffman, Plasma bubbles and irregularities in the equatorial ionosphere, *J. Geophys. Res.*, 82, 2650–2656, 1977.
- Mendillo, M., and A. Tyler, Geometry of depleted plasma regions in the equatorial ionosphere, *J. Geophys. Res.*, 88, 5778–5782, 1983.
- Rodriguez, P., Overview of the LASSII experiment on the Combined Release and Radiation Effects Satellite, *J. Spacecr. Rockets*, 29, 564–565, 1992.
- Shaw, R. R., and D. A. Gurnett, Whistlers with harmonic bands caused by multiple stroke lightning, *J. Geophys. Res.*, 76, 1851–1854, 1971.
- Singleton, D. G., The morphology of spread F occurrence over half a sunspot cycle, *J. Geophys. Res.*, 73, 295–308, 1968.
- H. C. Koons and J. L. Roeder, Space and Environment Technology Center, The Aerospace Corporation, Mail Stop M2-260, P.O. Box 92957, Los Angeles, CA 90009. (e-mail: harry.koons@aero.org; jim_roeder@mail2.aero.org)
- P. Rodriguez, Plasma Physics Division, Naval Research Laboratory, Mail Code 6755, Washington, D. C. 20375. (e-mail: rodriguez@nrlpla.nrl.navy.mil)

TECHNOLOGY OPERATIONS

The Aerospace Corporation functions as an "architect-engineer" for national security programs, specializing in advanced military space systems. The Corporation's Technology Operations supports the effective and timely development and operation of national security systems through scientific research and the application of advanced technology. Vital to the success of the Corporation is the technical staff's wide-ranging expertise and its ability to stay abreast of new technological developments and program support issues associated with rapidly evolving space systems. Contributing capabilities are provided by these individual Technology Centers:

Electronics Technology Center: Microelectronics, VLSI reliability, failure analysis, solid-state device physics, compound semiconductors, radiation effects, infrared and CCD detector devices, Micro-Electro-Mechanical Systems (MEMS), and data storage and display technologies; lasers and electro-optics, solid state laser design, micro-optics, optical communications, and fiber optic sensors; atomic frequency standards, applied laser spectroscopy, laser chemistry, atmospheric propagation and beam control, LIDAR/LADAR remote sensing; solar cell and array testing and evaluation, battery electrochemistry, battery testing and evaluation.

Mechanics and Materials Technology Center: Evaluation and characterization of new materials: metals, alloys, ceramics, polymers and composites; development and analysis of advanced materials processing and deposition techniques; nondestructive evaluation, component failure analysis and reliability; fracture mechanics and stress corrosion; analysis and evaluation of materials at cryogenic and elevated temperatures; launch vehicle fluid mechanics, heat transfer and flight dynamics; aerothermodynamics; chemical and electric propulsion; environmental chemistry; combustion processes; spacecraft structural mechanics, space environment effects on materials, hardening and vulnerability assessment; contamination, thermal and structural control; lubrication and surface phenomena; microengineering technology and microinstrument development.

Space and Environment Technology Center: Magnetospheric, auroral and cosmic ray physics, wave-particle interactions, magnetospheric plasma waves; atmospheric and ionospheric physics, density and composition of the upper atmosphere, remote sensing, hyperspectral imagery; solar physics, infrared astronomy, infrared signature analysis; effects of solar activity, magnetic storms and nuclear explosions on the earth's atmosphere, ionosphere and magnetosphere; effects of electromagnetic and particulate radiations on space systems; component testing, space instrumentation; environmental monitoring, trace detection; atmospheric chemical reactions, atmospheric optics, light scattering, state-specific chemical reactions and radiative signatures of missile plumes, and sensor out-of-field-of-view rejection.